Biomass Conversion and Biorefinery (2024) 14:19005–19015
https://doi.org/10.1007/s13399-023-04018-x

ORIGINAL ARTICLE

In vitro biological assessment of green synthesized iron oxide nanoparticles using *Anastatica hierochuntica* (Rose of Jericho)

Mahesh Vahini[1] · Sivakumar Sowmick Rakesh[1] · Rajakannu Subashini[1] · Settu Loganathan[2] · Dhakshinamoorthy Gnana Prakash[3]

Received: 20 December 2022 / Revised: 21 February 2023 / Accepted: 28 February 2023 / Published online: 7 March 2023

Abstract

Nanoparticle production can be done easily, safely and without using any harmful chemicals. Due to the multiple biomedical applications of iron oxide nanoparticles, the current study uses plant extracts of *Anastatica hierochuntica* (*A. hierochuntica*) for the environmental friendly production of iron oxide nanoparticles (IONPs). UV–visible spectroscopy, Fourier transform infrared (FT-IR) spectroscopy, X-ray diffraction (XRD), energy-dispersive X-ray analysis (EDAX) and scanning electron microscopy (SEM) were the methods utilized to investigate the formation of the iron oxide nanoparticles. In UV–visible analysis, absorption peaks of plant extracts of *A. hierochuntica* and biosynthesized IONPs were observed at 310 nm and 390 nm respectively. Functional groups such as alkenes, phosphate, carboxylic acid and hydroxyl groups were observed by the FT-IR study. The produced IONPs crystallinity was further confirmed by the XRD examination, and their average size was found to be 52 nm. SEM analysis revealed most of the formed nanoparticles were in spherical shape with 30–70-nm size. The presence of iron, oxygen, carbon and other elements was further confirmed in the EDAX spectrum. Five different bacteria *Staphylococcus aureus*, *Pseudomonas aeruginosa*, *Enterococcus faecalis*, *Bacillus subtilis* and *Escherichia coli* were tested for the biosynthesized IONP antibacterial efficacy. With an inhibitory zone measuring 28.32 ± 1.5 in diameter, the generated IONPs exhibited considerable antibacterial activity against the Gram-positive bacteria *Bacillus subtilis*. The percentage antioxidant activity of biosynthesized IONPs rises with an increasing concentration, and the highest activity of 36.79% was observed at the concentration of 100 µg/mL. In addition, the in vitro cytotoxicity studies against human breast cancer cell line MCF-7 showed that the cell viability of biosynthesized IONPs was hazardous to the MCF-7 cell line, with concentrations ranging between 7.8 and 1000 µg/mL, displaying the strongest and lowest anti-cancer activity, with IC50 value of 52.17%. The haemolytic activity of biosynthesized IONPs demonstrates that the rate of lysis steadily increased with increasing concentrations. At a high concentration of 1000 µg/mL, 24% of lysis and at a lower concentration of 31.25 µg/mL, 2.2% lysis was observed. The iron oxide nanoparticles produced by this biogenic method will therefore have more varied uses in the biomedical industry with further clinical evaluation.

Keywords *Anastatica hierochuntica* · Green synthesis · Iron-oxide nanoparticle · Antibacterial activity · DPPH antioxidant activity

1 Introduction

In recent years, scientists and researchers have concentrated on nanotechnology to produce nanoscale materials using various physicochemical and biological processes. A variety of industries including agriculture, sensors for hazardous gases, catalysts in wastewater treatment and medicinal applications use nanoparticles, which have sizes ranging from 1 to 100 nm [1]. The features of nanoparticles can be divided into two categories: As particle size decreases as a result of (i) surface effects or size reduction and (ii) quantum

✉ Rajakannu Subashini
subashinir@ssn.edu.in

[1] Department of Biomedical Engineering, Sri Sivasubramaniya Nadar College of Engineering, Kalavakkam, Chennai, Tamil Nadu 603110, India

[2] Department of Anatomy, Saveetha Dental College and Hospital, Saveetha Institute of Medical and Technical Sciences, Chennai, Tamil Nadu 600 007, India

[3] Department of Chemical Engineering, Sri Sivasubramaniya Nadar College of Engineering, Kalavakkam, Chennai, Tamil Nadu 603110, India

confinement effects, more atoms are found on the surface changes depending on a number of factors [2]. Vapour deposition, mechanical methods and chemical synthesis processes such as sol–gel, co-precipitation, hydrothermal, solvothermal and pyrolysis are examples of physical synthesis procedures for metal and metal oxide nanoparticles [3–5].

Researchers are exploring ecological friendly synthetic methodologies for nanoparticle manufacturing in order to get over the limits of physical and chemical procedures. An alternative to nanoparticle synthesis is green synthesis. This process avoids manufacturing toxic by-products and is efficient, sustainable and environmentally beneficial [6]. Metal nanoparticles are created using environmental friendly processes from biological components such as plant extracts, bacteria, fungi and algae. Plant extracts are frequently utilized to make metal oxide nanoparticles because it is a quick, affordable and straightforward process. Biological nanoparticles are another name for the nanoparticles created utilizing the green technique [1]. Modern nanostructures that are compatible with improvements in already created materials can be produced by a number of plants. Phytochemicals or secondary metabolites are abundant in plant biodiversity, especially in leaves. These include compounds phenols, flavonoids, terpenoids, amides, aldehydes and ketones [7]. These secondary metabolites convert the metal precursors into metal nanoparticles. The synthesis of environmental friendly metal nanoparticles is influenced by reaction variables such as solvent and precursor concentrations, reaction time, temperature, pressure and pH [8]. Therefore, it is essential to create environmentally secure nanoparticle synthesis methods. Compared to chemical and physical approaches, green synthesis offers a number of advantages: it is non-toxic, pollution-free, ecological friendly, inexpensive and more sustainable. This technology uses the raw material plant as both a capping and a reducing agent, which eliminates the need for dangerous chemicals. Consequently, biological nanoparticle synthesis using plant extracts is more bio-compatible than chemical synthesis [9]. Iron oxide is one of the most often used forms of iron in a variety of applications. It can be used as a photocatalyst in the photolysis of phenolic compounds, a CO sensor and other gas detector, an anode in batteries and in the pharmaceutical industry, among many other things [10, 11].

Anastatica hierochuntica (*A. hierochuntica*), often known as the Rose of Jericho, is the only known species in the Anastatica genus and a well-known medicinal plant in the Brassicaceae family [10]. Plants are developed from seeds during the brief wet season, rarely higher than 15 cm, its tiny white blossoms. The stem bends inward into a dense hardwood ball with a diameter of 4 to 10 cm after the wet season, when the plant dries up. Because they are tough, seeds can hibernate for long periods of time. Tea prepared from this is used to treat all of these ailments including typhoid fever, salmonella typhoid, dysentery, diabetes, headaches and heart disease. The therapeutic benefits of this plant are due to its phytochemical components [12]. This category also includes alcoholic and aqueous extracts of carbohydrates, phenols, flavonoids, tannins, saponins and alkaloids of the same composition in addition to *n*-hexane extracts that include phenols, terpenoids and sterols. It has several physiological effects on the human body [13, 14]. Antioxidant, antibacterial, antifungal, hypolipidaemic and hypoglycaemic activities are induced by the extracts of *A. hierochuntica* [15–17]. In the present study, iron oxide nanoparticles were made using extracts of *A. hierochuntica* plant, and its antibacterial, antioxidant, cytotoxic and haemolytic properties were examined.

2 Materials and methods

Ferric chloride (98%), ferrous sulphate heptahydrate (98%), ethanol, NaOH and bacterial growth media were purchased from Sigma-Aldrich. The *Anastatica hierochuntica* (Rose of Jericho) plant was obtained from Raw Herbs India Pvt. Ltd.

2.1 Extraction of aqueous plant of *A. hierochuntica*

The selected therapeutic plant *A. hierochuntica* was dried at shade and chopped into pieces. A mortar and pestle were used to pulverize the chopped herb into fine powder. The aqueous extract of the herb was prepared as per previously described method by Mohammd et al. [18] with slight changes. Accordingly, 10 g of herbal powder thoroughly mixed with 100 mL of distilled water and the mix was incubated for 30 min at 80 °C at atmospheric pressure. The incubated mix was then filtered using Whatman grade no. 1 filter paper to collect the filtered-out fluid (extract), and this extract was concentrated using a rotary evaporator at normal temperature and pressure. The prepared aqueous *A. hierochuntica* plant extract was then stored at – 20 °C for further studies. This extraction process is repeatable by strictly following the same parameters and procedures. Additionally, UV–Visible spectroscopic analysis was performed for the sample diluted to 1:10 ratio with distilled water to verify the active ingredients present in the extract of *A. hierochuntica*.

2.2 Fabrication of iron-oxide nanoparticle using *A. hierochuntica*

Iron oxide nanoparticles from *A. hierochuntica* were synthesized in an aqueous solution of 20-mL (0.1 M) ferrous sulphate heptahydrate ($FeSO_4 \cdot 7H_2O$) and 20-mL (0.1 M) ferric chloride solution ($FeCl_3$) to 30 mL of plant extract at room temperature. The standard NaOH solution (0.1 N) was used to maintain the pH of the synthesized reaction mixture

at 9. The reaction mixture changes to dark brown from yellow after 3 h of nonstop stirring. The nanoparticles were separated by centrifuging the reaction mixture at 10,000 rpm for approximately 10 min [9]. Isolated nanoparticles were collected in an airtight container for additional preservation.

2.3 Characterization of iron oxide nanoparticles

2.3.1 Ultraviolet–visible spectroscopy

The characteristics of aqueous plant extract and bioderived iron oxide nanoparticles were determined by UV–Visible spectroscopic analysis. The analysis was done by using JascoV-630, and the sample was scanned between 200 and 800 nm at a scanning speed of 300 nm/min [9]. The colour formation of plant extract and iron oxide nanoparticles by the activation of surface plasmon resonance was examined. Using a Milli-Q water purification system, distilled and deionized (DI) water was used to prepare the blanks.

2.3.2 FT-IR analysis

The functional groups in biomolecules that are present in biosynthesized IONPs were observed in Fourier transform infrared (FT-IR) spectroscopy [19]. The biosynthesized IONPs were scanned in the 400–4000 cm^{-1} range on a PerkinElmer FTIR spectrometer.

2.3.3 XRD analysis

An X-ray diffraction (XRD) analysis has been used to measure the size of the formed iron oxide nanoparticles (IONPs). XRD measurements was performed using a Shimadzu 7000 power X-ray diffractometer in scan mode with continuous scans ranging from 20° to 80° and monochromatic Cu-Ka radiation ($k = 1.5406$) at room temperature [20]. The size of the IONPs was calculated from the highest peak.

2.3.4 SEM and EDAX

Morphology and size of the formed nanoparticles were analysed using scanning electron microscope (SEM) (Model Jeol 6390LA/ OXFORD XMX N). In addition, metal elemental components (iron) were detected by energy dispersive X-ray (EDAX) spectrometer [9].

2.4 Antibacterial activity

Nanoparticles, which have been thoroughly studied for their antibacterial properties, may be a feasible choice for the production of pharmaceuticals, used in therapeutic applications. Antibacterial activity against disease causing microorganisms such as *Staphylococcus aureus*, *Pseudomonas aeruginosa*, *Enterococcus*, *Bacillus subtilis* and *Escherichia coli* was done using the agar disc diffusion method. Ciprofloxacin antibiotic discs were utilized as positive control. The temperature of stock cultures was kept constant at 4 °C on nutrient agar slants. Active experimental cultures were prepared using the transferring one loop of culture from stock cultures to broth tubes and incubating at 37 °C for 24 h [21]. In Muller Hinton Agar (MHA) medium, the antibacterial properties of the sample were studied using the disc diffusion technique. A Petri dish was filled with MHA medium (10–15 mL). After the medium had set for 10–15 min, the inoculum was applied to the surface using a sterile swab dipped in the bacterial solution. Using forceps, the disc was inserted into the MHA plate together with 20 µL of biosynthesized IONPs (concentrations of 1000 µg/mL, 750 µg/mL, and 500 µg/mL). Plates were incubated at a temperature of 37 °C for 24 h. The diameter of the zone of inhibition was then used to examine the antibacterial activity.

2.5 Antioxidant activity

A free radical scavenging test called the diphenyl-1-picrylhydrazyl (DPPH) assay was carried out on the biosynthesized IONPs to ascertain its antioxidant capacity [22, 23]. Freshly prepared DPPH solution (0.004%w/v) was added in each test tube containing biosynthesized IONPs at the concentration of 20 µg/mL, 40 µg/mL, 60 µg/mL, 80 µg/mL and 100 µg/mL. Ninety-five per cent methanol was used as blank. After the samples had been incubated in the dark for roughly 30 min, the samples' absorbance was measured at 517 nm. The following formula was used to calculate the free radical scavenging percentage:

$$\%\ \text{Antioxidant activity} = \frac{(\text{Absorbance of blank}) - (\text{Absorbance of test})}{(\text{Absorbance of blank})} \times 100$$

2.6 Cytotoxic activity

The MCF 7 cell line, which is used to study breast cancer, was cultured in DMEM with 10% foetal bovine serum, 100 µg/mL penicillin and 100 µg/mL streptomycin in a humidified environment with 50 µg/mL CO_2 at 37 °C. It was multiplied by seeding cells in 24-well plates and incubating them under 37 °C, 5% CO_2 conditions. Different sample concentrations (7.8 µg/mL, 15.6 µg/mL, 31.2 µg/mL, 62.5 µg/mL, 125 µg/mL, 250 µg/mL, 500 µg/mL, 1000 µg/mL) were added once the cells had reached confluence, and the mixture was then incubated for 24 h [24]. Samples were taken out of the wells and rinsed with DMEM without serum after incubation. One hundred microliters per millilitre per well for 4 h was spent

incubating with 0.5% 3-(4,5-dimethyl-2-thiazolyl)-2,5-diphenyl-tetrazolium bromide (MTT). All wells received 1 mL of DMSO after incubation. DMSO was used as a blank in a UV spectrophotometer to assess absorbance at 570 nm. The concentration necessary for 50% inhibition (IC50) was plotted after measurements were made. The % cell viability was calculated using the following formula:

$$\%\ \text{Cell viability} = \frac{\text{Absorbance of treated cells}}{\text{Absorbance of control cells}} \times 100$$

2.7 Haemolytic activity

The compatibility of biosynthesized IONPs was carried out using haemolytic assay with freshly separated red blood cells. The RBCs are separated from the blood by centrifugation method at 14,000 rpm for 5 min. The suspension of RBCs was prepared in phosphate buffer solution (PBS) at pH 7.4 by adding 200 µL of RBC to 6 mL PBS. The biosynthesized IONP concentration 100 µg/mL was mixed with erythrocyte suspension and incubated at 25 °C for 4 h. The test samples were then centrifuged at 10,000 rpm for 10 min. The supernatant was collected, and absorbance was recorded at 545 nm [25]. Triton X 100 (2%) served as positive and DMSO as negative controls. The haemolysis percentage was calculated using the formula below:

$$\text{Hemolysis}\ (\%) = \frac{\text{Sample OD} - \text{Negative control}}{\text{Positive Control} - \text{Negative control}} \times 100$$

3 Results and discussions

3.1 Ultraviolet–visible spectroscopy

The IONPs synthesized from aqueous extract of *A. hierochuntica* were indicated by the colour change from yellow to brown. The plant extract and iron oxide nanoparticle formation is confirmed with the presence of distinctive peaks at 310 nm and 390 nm respectively, because synthesized nanoparticles are said to be distinguished by the excitation of surface plasmon resonance as shown in Fig. 1. Similar research for UV–Visible analysis has been reported with the green synthesis of iron oxide particles by Kirdat et al. [3].

3.2 FT-IR

Figure 2 depicts the Fourier transform infrared spectroscopy (FT-IR) spectra of the biosynthesized IONPs

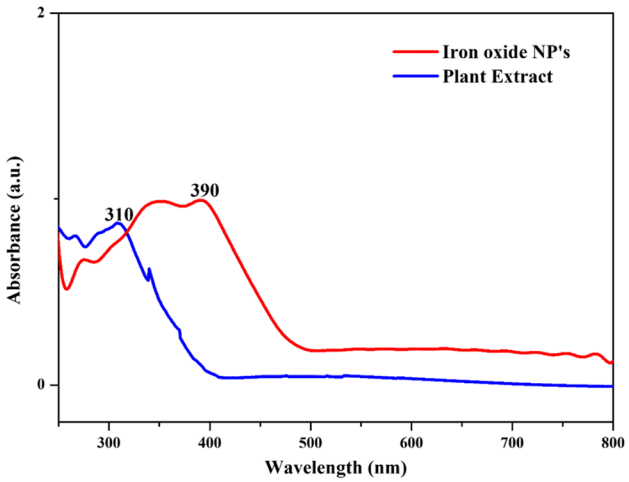

Fig. 1 UV–visible spectrum of IONPs and extracts of *A. hierochuntica*

using *A. hierochuntica*. The transmittance peak for the biosynthesized IONPs is observed at 682.79 cm^{-1}, 1016.88 cm^{-1}, 3201.58 cm^{-1} and 3848.32 cm^{-1}. The stretching at 682.79 cm^{-1} reveals the existence of alkenes. The phosphate ion was present as shown by the stretching at 1016.88 cm^{-1} [26]. The peaks at 3201.58 cm^{-1} correspond to O–H bond stretching vibration of alcohol and phenol group while 3848.32 cm^{-1} represents hydroxyl group. The peaks shifting indicate bio-reduction and stabilization by the phytochemicals included in the IONPs that were produced by biological synthesis. The FT-IR analysis thus revealed the locations where interactions of extract molecules with iron metal ions [27].

3.3 XRD

To ascertain the crystallinity and surface morphology of the produced IONPs, X-ray diffraction (XRD) examinations were carried out at 2 theta angles ranging from 20° to 80°. The XRD data in Fig. 3 reveals the (220), (311), (400), (401), (422) and (214) crystal planes at 31.69°, 35.68°, 43.40°, 45.50°, 56.45° and 62.83° respectively. This specifies the presence of synthesized iron oxide bionanoparticles. Based on the strong and prominent peaks, the Fe_2O_3 nanoparticles produced by the reduction procedure using extract from *A. hierochuntica* were unquestionably crystalline. These XRD findings for iron oxide nanoparticles are roughly the same as those made by other researchers [28, 29]. The Debye–Scherrer equation was applied to XRD analyses to measure the size of the produced biosynthesized iron oxide nanoparticles. The average crystallite size as calculated using the Debye–Scherrer equation ($D_{XRD} = (K\ \lambda/\beta\ \cos\ \theta)$) was found to be 52 nm.

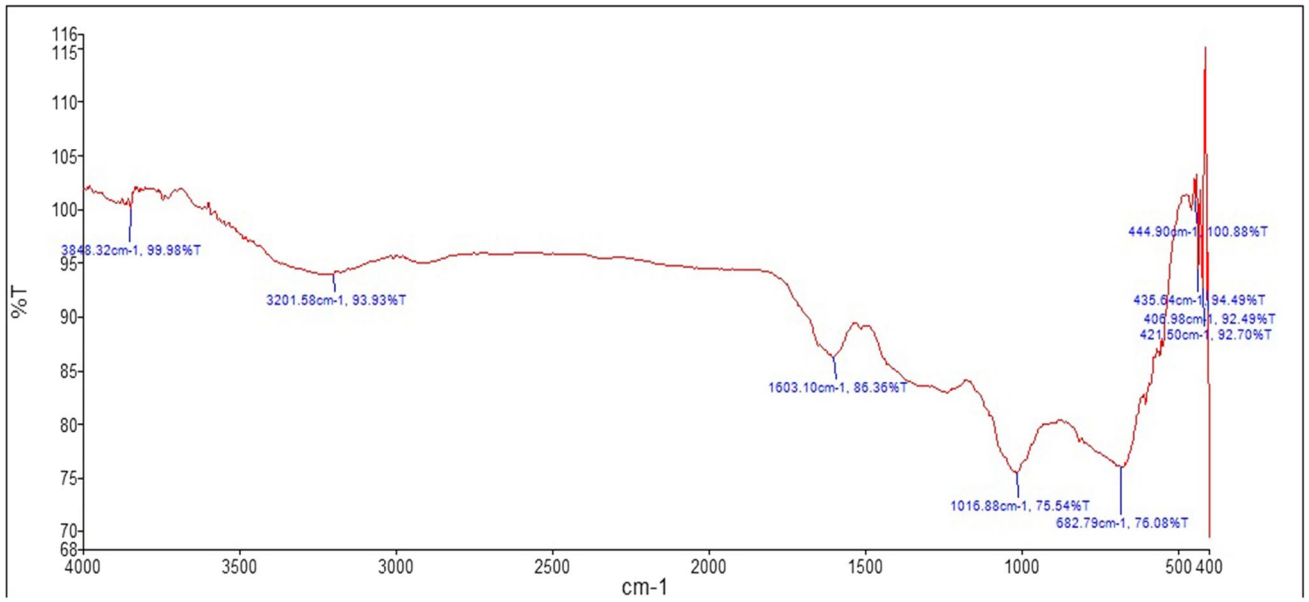

Fig. 2 FT-IR spectrum of biosynthesized IONPs using *A. hierochuntica*

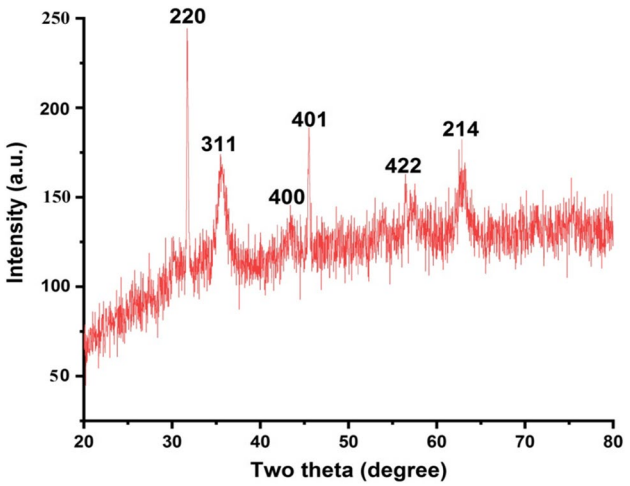

Fig. 3 XRD analysis of biosynthesized IONPs using *A. hierochuntica*

3.4 SEM

The SEM images of the biosynthesized IONPs at different magnifications are represented in Fig. 4a–c. SEM images exposed that IONPs were synthesized successfully. The mean particle size of the synthesized IONPs was determined to be in the range of 30–70 nm by the Image J software program. As seen from Fig. 4a–c, most of the formed nanoparticles were spherical and few were in cubic morphologies. Similar to the present study, Jagathesan and Rajiv reported that *Eichhornia crassipes* leaf extract–mediated IONPs were spherical in shape confirmed by SEM analysis [30]. Figure 5 depicts the EDAX image of biosynthesized iron oxide nanoparticles. The elemental composition of IONPs is analysed using EDAX, and it was found to be 44.16% of iron, 19.16% of oxygen and 19.87% of sodium and presence of other elements. A similar spectrum has been shown by Velsankar K et al. [31].

3.5 Antibacterial activity

The agar disc diffusion method was used to screen biosynthesized IONPs and positive control ciprofloxacin for antibacterial activity against *Staphylococcus aureus*, *Pseudomonas aeruginosa*, *Enterococcus faecalis*, *Bacillus subtilis* and *Escherichia coli*. This study demonstrated that when the concentration of the produced IONPs increases, their antibacterial activity also increases similar to the study by Biswas et al. [21]. Table 1 depicts the antibacterial activity of biosynthesized IONPs, and Fig. 6 illustrates the inhibitory ability of the IONPs against the test organism after 24 h of incubation. The produced bionanoparticles have a 28.32 ± 1.5 mm diameter inhibitory zone and exhibited strong antibacterial activity at 1000 µg/mL concentration against *Bacillus subtilis*. It was clear from the mean zone of inhibition, IONPs at concentrations of 1000 µg/mL, 750 µg/mL, and 500 µg/mL inhibited *Bacillus subtilis* more effectively than *Staphylococcus aureus*, *Pseudomonas aeruginosa*, *Enterococcus faecalis* and *Escherichia coli*. The antibacterial mechanism against bacillus and also other bacterial species may be due to number of different processes. The primary proposed mechanism is the reactive oxygen species (ROS) generate oxidative stress [32]. Hydrogen peroxide Singlet oxygen, superoxide radicals and hydroxyl radicals

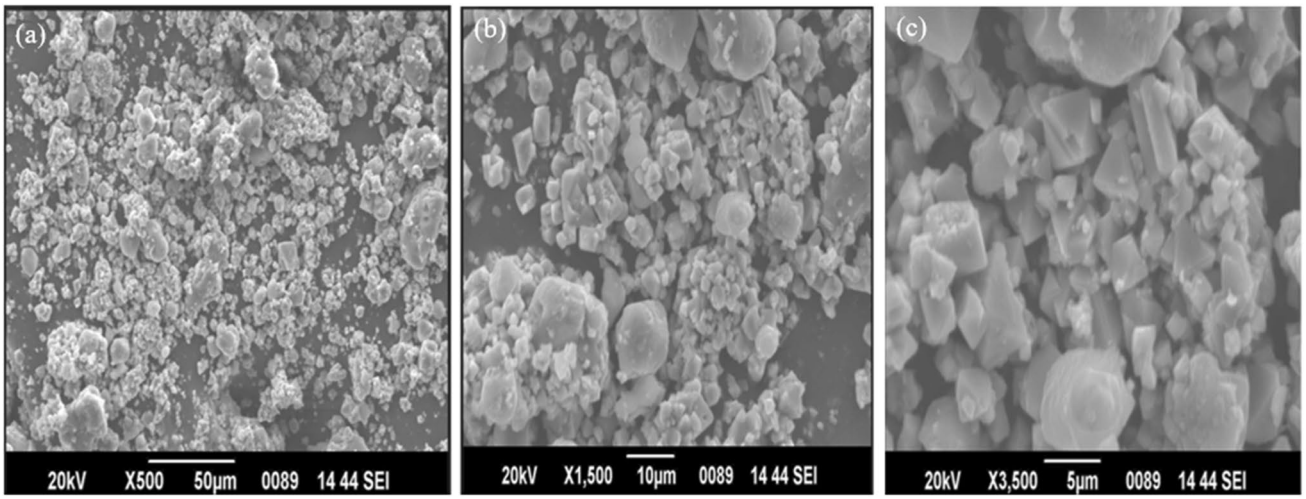

Fig. 4 SEM images of IONPs at different magnifications (**a**–**c**)

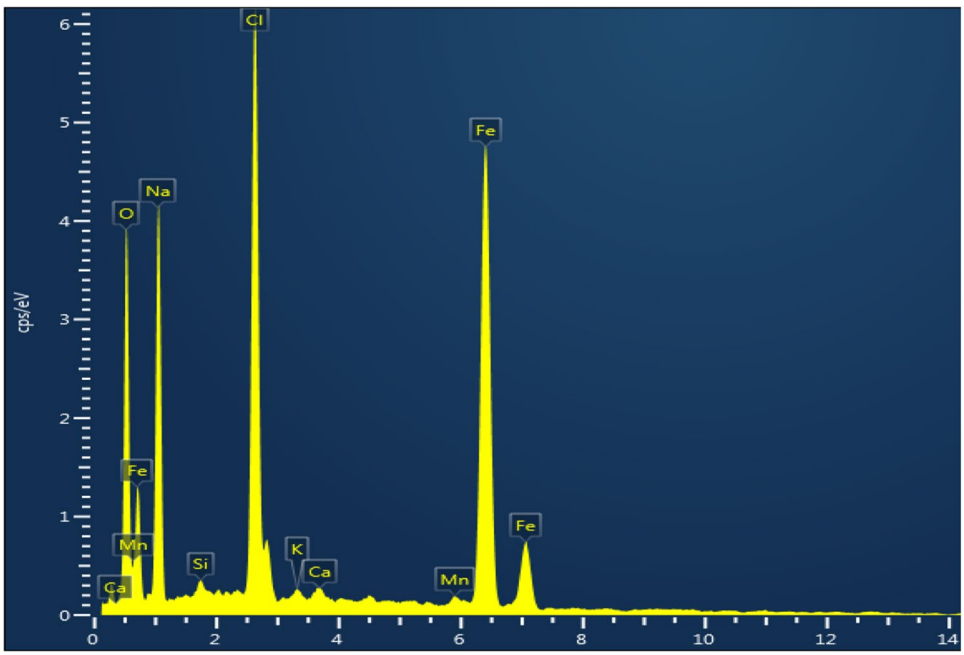

Fig. 5 EDAX image of biosynthesized iron oxide nanoparticles

Table 1 Antibacterial activity of biosynthesized IONPs using *A. hierochuntica*

Organisms	Zone of Inhibition (mm)			
	IONPs concentrations (µg/ mL)			Ciprofloxacin (1 mg/mL)
	1000	750	500	
S. aureus	8.43 ± 2.0	7.21 ± 1.5	7.03 ± 0.5	34.23 ± 1.8
P. aeruginosa	8.32 ± 1.5	8.16 ± 1.0	8.24 ± 0.5	9.41 ± 1.0
E. faecalis	15.10 ± 1.5	8.25 ± 1.0	7.36 ± 0.5	32.14 ± 1.5
B. subtilis	28.32 ± 1.5	14.1 ± 0.5	9.49 ± 1.0	47.33 ± 1.3
E. coli	8.22 ± 1.0	7.41 ± 1.5	7.32 ± 0.5	7.24 ± 0.9

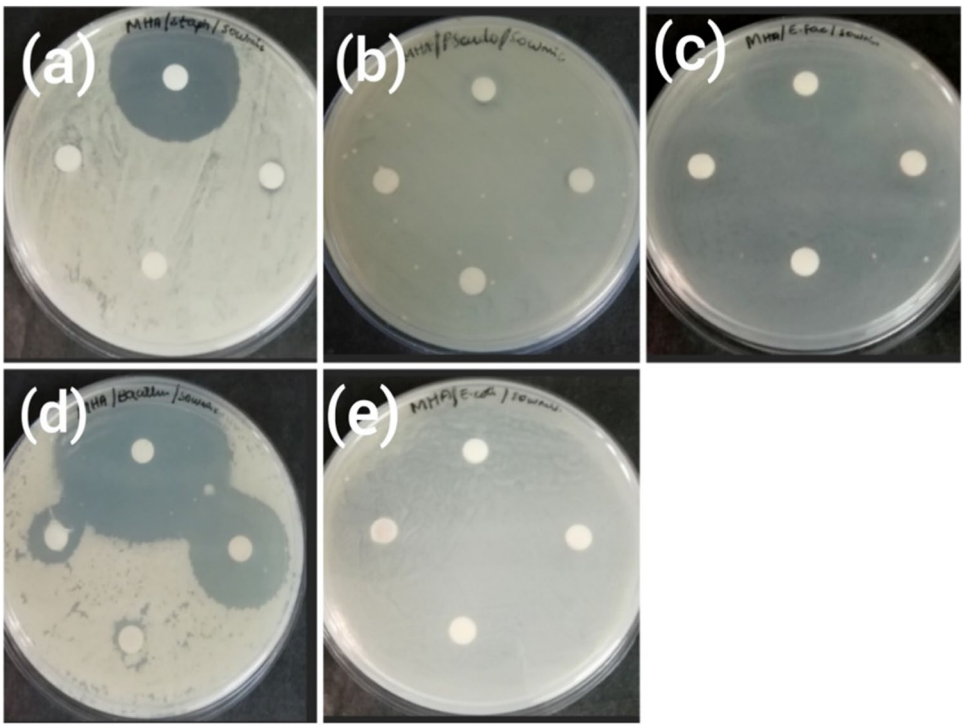

Fig. 6 Antibacterial activity, zone of inhibition (ZOI) caused by biosynthesized IONPs using *A. hierochuntica* against five pathogenic bacteria **a** *Staphylococcus aureus*, **b** *Pseudomonas aeruginosa*, **c** *Enterococcus faecalis*, **d** *Bacillus subtilis*, **e** *Escherichia coli*

are examples of ROS that can harm bacteria's DNA and proteins chemically [33]. Secondary physical harm caused by electrostatic interactions between nanoparticles and bacterial cell membranes or cell membrane proteins can result in the death of the bacteria [34]. Other research has shown that small size and high surface area to volume ratio allow the iron oxide nanoparticle to interact with the membrane of the bacteria. The biosynthesized IONPS using *A. hierochuntica* showed higher activity against *E. coli* which is reflected in the mean zone values of 8.22 ± 1.0 mm at maximum concentration. The recorded activity is higher than that of the standard ciprofloxacin (7.24 ± 0.9 mm). This bactericidal effect could be due to the smaller size of IONPs. According to Arokiyaraj et al. [32], the killing of *E. coli* by zero-valent iron nanoparticles may be caused by the diffusion of the tiny particles (sized between 10 and 80 nm) into the membranes of *E. coli*, which produces oxidative stress and ruptures the cell membrane.

3.6 Antioxidant activity

According to the DPPH free radical assay, the produced biosynthesized IONPs have a higher antioxidant potential which shows their capacity to capture free radicals. The

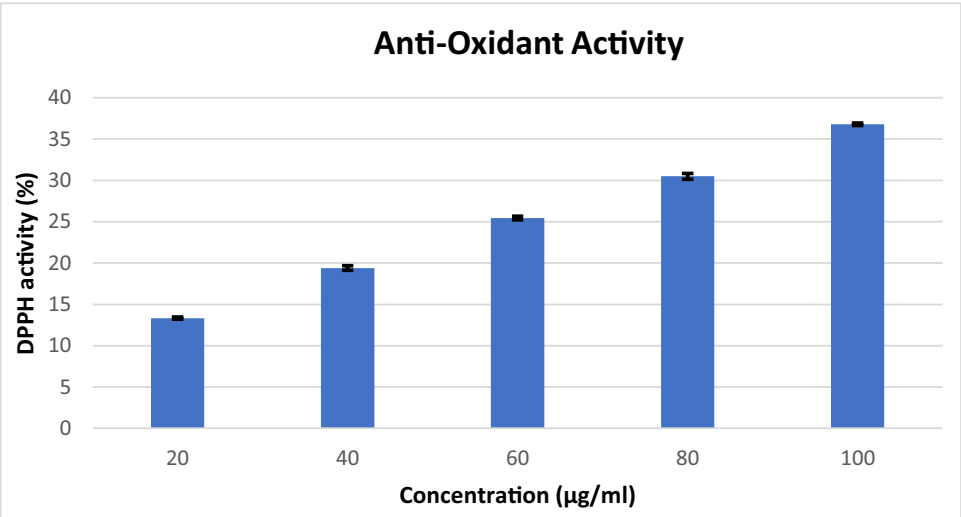

Fig. 7 DPPH free radical scavenging activity of biosynthesized IONPs using *A. hierochuntica*. Values are presented as mean ± SD ($n = 3$)

effect of different concentrations of biosynthesized IONPs on DPPH scavenging activity is shown in Fig. 7. The DPPH activity of biosynthesized IONPs was found to increase in a dose-dependent manner, with 100 µg/mL producing the highest maximum activity inhibition of 36.79% and 20 µg/mL producing the lowest minimum activity inhibition of 13.33%. The DPPH radical test clearly demonstrates that biosynthesized iron oxide nanoparticles have a better antioxidant capacity and are capable of donating a free radical to eliminate the old electron that is responsible for the free radical reactivity. Similar to the study of Abdullah et al. [23], it was found in the current investigation that when IONP concentration increases, so does their antioxidant activity. Similar research on the improved antioxidant capabilities of biosynthesized Ag-NPs and CuNPs from plant sources such as *Aegle marmelos* [35] and *Withania somnifera* [22] has been reported.

3.7 Cytotoxic activity

MTT colorimetric assay was performed to assess the cytotoxic activity of the green synthesized iron oxide nanoparticles using *A. hierochuntica.* The untreated cells served as a control (100% viability). The present finding exposed that the nanoparticles significantly inhibited the growth of MCF-7 cells in a dose/concentration-dependent manner. The

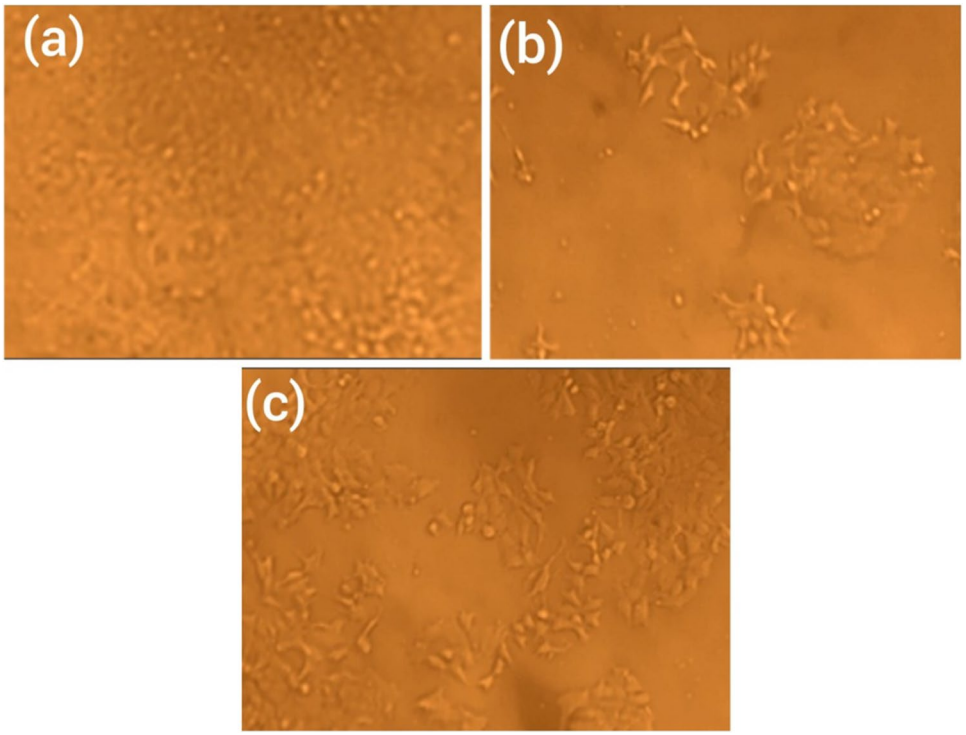

Fig. 8 Cytotoxic effect of biosynthesized IONPs using *A. hierochuntica* on MCF 7 cell line. **a** Normal MCF 7 cell line, **b** 1000 µg/mL, **c** 7.8 µg/mL

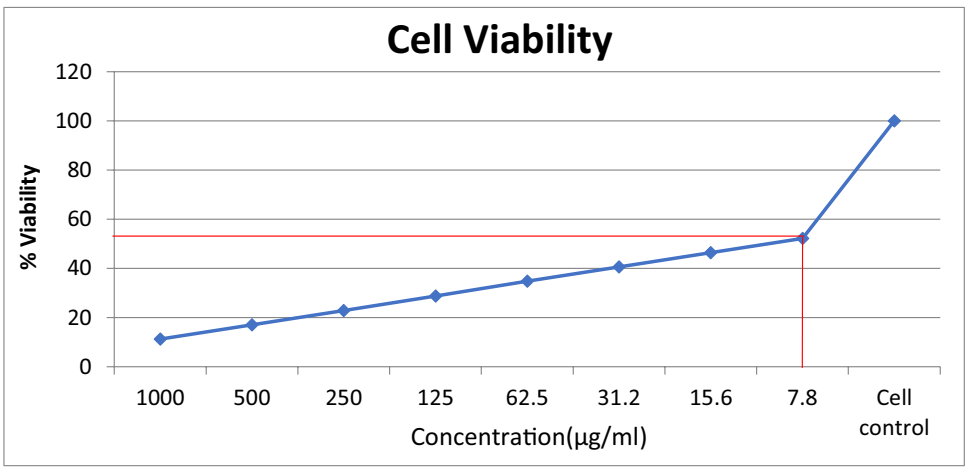

Fig. 9 Effect of biosynthesized IONPs on cell viability in dose-dependent manner

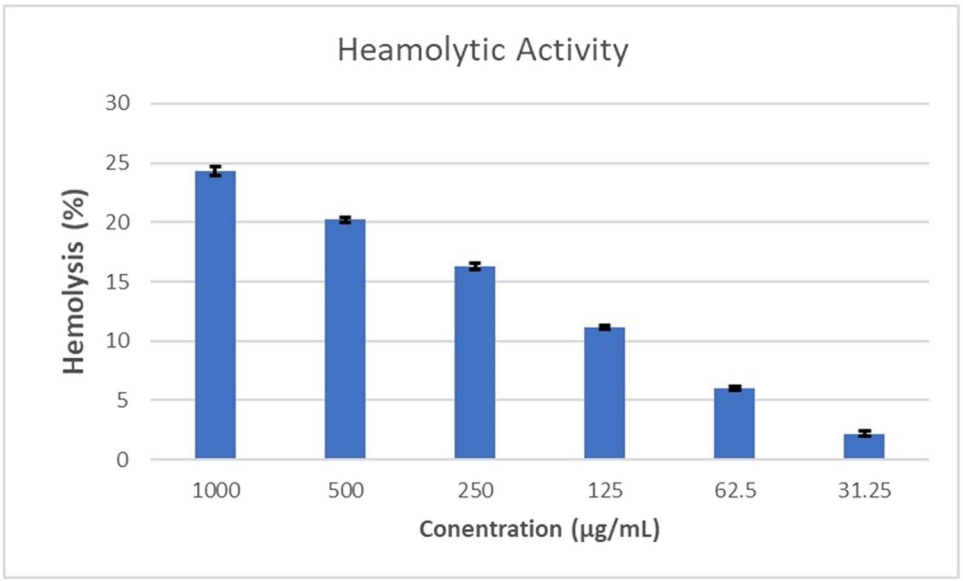

Fig. 10 Haemolytic activities of biosynthesized IONPs using *A. hierochuntica*

cytotoxicity of biosynthesized IONPs against the MCF-7 cell line was proven in our work using the MTT assay, with the highest and lowest anti-cancerous activities at concentrations 1000 µg/mL and 7.8 µg/mL as shown in Fig. 8a, b, c. The inhibitory concentration IC_{50} was found to be 7.8 µg/mL with the inhibition of 52.17% for 24-h treatment as shown in Fig. 9. It is clearly evident from the obtained results that at a very low concentration of 7.8 µg/mL, the cell survival was reduced to nearly half (52.17%), and as the concentration increases, the cell viability decreases appreciably. Nagajyothi et al. [24] reported that the cytotoxic ability of iron oxide nanoparticles with clear concentration-dependent cell growth inhibition on MCF-7 breast cancer cells. Abouelella et al. [36] reported extracts of *A. hierochuntica*, registered excellent cytotoxic activities against HeLa cell lines. In a different investigation, Erdogan et al. reported that red cabbage peel extract–mediated IONPs reduced the viability of MCF-7 cells to roughly 72.5% at concentrations of 1, 10, 100 and 1000 µg/mL [37]. The present work reported toxicity of biosynthesized IONPs against MCF-7 cells is remarkably high at low concentration similar to these previous findings.

3.8 Haemolytic activity

To study the toxicity of biosynthesized IONPs on erythrocytes, haemolytic activity is performed at concentrations of biosynthesized IONPs ranging between 1000 and 31.25 µg/mL according to Hassan et al. [25]. The results indicated that at high concentration of IONPs (1000 µg/mL), highest haemolysis was observed at 24%, while at low concentration of IONPs (31.25 µg/mL), lowest haemolysis was observed at 2.2% as shown in Fig. 10. According to "American Society for Testing and Materials Designation" materials with < 2% is non-haemolytic [38]. Therefore, our results indicate a non-haemolytic behaviour at low concentrations of 31.25 µg/mL, and this can be categorized as non-haemolytic concentration and biocompatible to that of RBC.

4 Conclusion

In the present study, iron oxide nanoparticle was successfully created biologically using the extract from *A. hierochuntica.* The generated bionanoparticles were examined using XRD, FT-IR and UV–visible spectroscopy techniques. It exhibits a recognizable absorption peak in the UV–visible spectrum at 390 nm, and FT-IR analysis identifies a number of functional groups. The average size of nanoparticles as determined by XRD analysis is 52 nm, and this measurement again supported the crystalline character of the produced IONPs. SEM images showed that the average size of iron oxide nanoparticles was 30–70 nm. The effectiveness of the produced biosynthesized IONPs, inhibiting bacterial growth, was also examined with the different pathogenic bacteria. Antibacterial assay showed that the biosynthesized iron oxide nanoparticles have good activity against *B. subtilis* and *E. coli.* The antioxidant activity increases with increasing concentration of biosynthesized IONPs by DPPH assay. The biosynthesized IONPs exhibited cytotoxic activity against MCF-7 breast cancer cell lines. Hence, the findings of present study are anticipated to provide new avenues in the biomedical applications for the clinical development of novel therapeutic agent against infectious diseases.

Acknowledgements The authors are thankful to the management of Sri Sivasubramaniya Nadar College of Engineering, Kalavakkam, Chennai, Tamil Nadu, for providing the necessary infrastructural facilities for the current research work.

Author contribution Mahesh Vahini and Sivakumar Sowmick Rakesh: investigation, conceptualization, methodology, writing original draft. Rajakannu Subashini: conceptualization, data curation, writing original draft. Settu Loganathan and Dhakshinamoorthy Gnana Prakash: formal analysis, data curation.

Funding This work was funded by Sri Sivasubramaniya Nadar College of Engineering, Kalavakkam, Chennai, Tamil Nadu.

Data availability The data used to support the finding of this study are included within the manuscript.

Declarations

Ethics approval Not applicable.

Competing interests The authors declare no competing interests.

References

1. Dikshit PK, Kumar J, Das AK, Sadhu S, Sharma S, Singh S, Gupta PK, Kim BS (2021) Green synthesis of metallic nanoparticles: applications and limitations. Catalysts 11(8):902. https://doi.org/10.3390/catal11080902
2. Campos EA, Pinto DV, Oliveira JI, Mattos ED, Dutra RD (2015) J Aerosp Technol Manag 7:267–276. https://doi.org/10.5028/jatm.v7i3.471
3. Kirdat PN, Dandge PB, Hagwane RM, Nikam AS, Mahadik SP, Jirange ST (2021) Synthesis and characterization of ginger (Z. officinale) extract mediated iron oxide nanoparticles and its antibacterial activity. Mater Today Proc 43:2826–2833. https://doi.org/10.1016/j.matpr.2020.11.422
4. Dusane PR, Gavhane DS, Kolhe PS, Bankar PK, Thombare BR, Lole GS, Kale BB, More MA, Patil SI (2021) Controlled decoration of palladium (Pd) nanoparticles on graphene nanosheets and its superior field emission behavior. Mater Res Bullet 140:111335. https://doi.org/10.1016/j.materresbull.2021.111335
5. Balakarthikeyan R, Santhanam A, Anandhi R, Vinoth S, Al-Baradi AM, Alrowaili ZA, Al-Buriahi MS, Kumar KD (2021) Fabrication of nanostructured NiO and NiO: Cu thin films for high-performance ultraviolet photodetector. Optic Mater 120:111387. https://doi.org/10.1016/j.optmat.2021.111387
6. Kanase RS, Karade VC, Kollu P, Sahoo SC, Patil PS, Kang SH, Kim JH, Nimbalkar MS, Patil PB (2020) Evolution of structural and magnetic properties in iron oxide nanoparticles synthesized using Azadirachta indica leaf extract. Nano Express 1(2):020013. https://doi.org/10.1088/2632-959X/aba682
7. Kumar JA, Prakash P, Krithiga T, Amarnath DJ, Premkumar J, Rajamohan N, Vasseghian Y, Saravanan P, Rajasimman M (2022) Methods of synthesis, characteristics, and environmental applications of MXene: a comprehensive review. Chemosphere 286:131607. https://doi.org/10.1016/j.chemosphere.2021.131607
8. Rajagopal A, Rajakannu S (2022) Cassia auriculata and its role in infection/inflammation: a close look on future drug discovery. Chemosphere 287:132345. https://doi.org/10.1016/j.chemosphere.2021.132345
9. Ahmad W, Kumar Jaiswal K, Amjad M (2021) Euphorbia herita leaf extract as a reducing agent in a facile green synthesis of iron oxide nanoparticles and antimicrobial activity evaluation. Inorg Nano-Metal Chem 51(9):1147–1154. https://doi.org/10.1080/24701556.2020.1815062
10. Zin SR, Kassim NM, Alshawsh MA, Hashim NE, Mohamed Z (2017) Biological activities of Anastatica hierochuntica L.: a systematic review. Biomed Pharmacother 91:611–620. https://doi.org/10.1016/j.biopha.2017.05.011
11. Wei H, Xue Q, Li A, Wan T, Huang Y, Cui D, Pan D, Dong B, Wei R, Naik N, Guo Z (2021) Dendritic core-shell copper-nickel alloy@ metal oxide for efficient non-enzymatic glucose detection. Sensors Actuators B: Chem 337:129687. https://doi.org/10.1016/j.snb.2021.129687
12. Biset G, Woday A (2021) Epilepsy treatment outcomes in the referral hospitals of northeast Ethiopia. Epilepsy Res 171:106584. https://doi.org/10.1016/j.eplepsyres.2021.106584
13. AlGamdi N, Mullen W, Crozier A (2011) Tea prepared from Anastatica hirerochuntica seeds contains a diversity of antioxidant flavonoids, chlorogenic acids and phenolic compounds. Phytochemistry 72(2–3):248–254. https://doi.org/10.1016/j.phytochem.2010.11.017
14. Zin SR, Kassim NM, Mohamed Z, Fateh AH, Alshawsh MA (2019) Potential toxicity effects of Anastatica hierochuntica aqueous extract on prenatal development of Sprague-Dawley rats. J Ethnopharmacol 245:112180. https://doi.org/10.1016/j.jep.2019.112180
15. Mohamed AA, Khalil AA, El-Beltagi HE (2010) Antioxidant and antimicrobial properties of kaff maryam (Anastatica hierochuntica) and doum palm (Hyphaene thebaica). Grasas Aceites 61(1):67–75. https://doi.org/10.3989/gya.064509
16. El Sayed RA, Hanafy ZE, Abd El Fattah HF, Mohamed AK (2020) Possible antioxidant and anticancer effects of plant extracts from Anastatica hierochuntica, Lepidium sativum and Carica papaya against Ehrlich ascites carcinoma cells. Cancer Biol 10(1):1–6. https://doi.org/10.7537/marscbj100120.01
17. Mahmoud TY, Ramadhan RS (2021) Effect of Anastatica hierochuntica on balancing fertility hormones of albino male mice. Ann Rom Soc Cell Biol 12:3892–3902. https://doi.org/10.3390/2Fnu13092973
18. Mohammd TU, Baker RK, Al-Ameri KA, Abd-Ulrazzaq SS (2015) Cytotoxic effect of aqueous extract of Anastatica hierochuntica L. on AMN-3 cell line in vitro. Grasas Aceites 61:67–75
19. Aisida SO, Ugwu K, Akpa PA, Nwanya AC, Nwankwo U, Bashir AK, Madiba IG, Ahmed I, Ezema FI (2021) Synthesis and characterization of iron oxide nanoparticles capped with Moringa Oleifera: the mechanisms of formation effects on the optical, structural, magnetic and morphological properties. Mater Today: Proc 36:214–218. https://doi.org/10.1186/s13104-022-06039-7
20. Zimmermann DD, Janka O, Buyer C, Niewa R, Schleid T (2021) Nd5OF5Se4 and Sm5OF5Se4: new layered oxide fluoride selenides of the lanthanoids. Solid State Sci 116:106601. https://doi.org/10.1016/j.solidstatesciences.2021.106601
21. Biswas A, Vanlalveni C, Lalfakzuala R, Nath S, Rokhum L (2021) Mikania mikrantha leaf extract mediated biogenic synthesis of magnetic iron oxide nanoparticles: characterization and its antimicrobial activity study. Mater Today: Proc 42:1366–1373. https://doi.org/10.26434/chemrxiv.13203887.v1
22. Shanmugapriya J, Reshma CA, Srinidhi V, Harithpriya K, Ramkumar KM, Umpathy D, Gunasekaran K, Subashini R (2022) Green synthesis of copper nanoparticles using Withania somnifera and its antioxidant and antibacterial activity. J Nanomater. https://doi.org/10.1155/2022/7967294
23. Abdullah JA, Jiménez-Rosado M, Guerrero A, Romero A (2022) Gelatin-based biofilms with FexOy-NPs incorporated for antioxidant and antimicrobial applications. Materials 15(5):1966. https://doi.org/10.1016/j.scp.2020.100280
24. Nagajyothi PC, Pandurangan M, Kim DH, Sreekanth TV, Shim J (2017) Green synthesis of iron oxide nanoparticles and their catalytic and in vitro anticancer activities. J Cluster Sci 28:245–257. https://doi.org/10.1007/s10876-016-1082-z

25. Hassan D, Khalil AT, Saleem J, Diallo A, Khamlich S, Shinwari ZK, Maaza M (2018) Biosynthesis of pure hematite phase magnetic iron oxide nanoparticles using floral extracts of Callistemon viminalis (bottlebrush): their physical properties and novel biological applications. Artif Cells 46(sup1):693–707. https://doi.org/10.1080/21691401.2018.1434534
26. Buarki F, AbuHassan H, Al Hannan F, Henari FZ (2022) Green synthesis of iron oxide nanoparticles using Hibiscus rosa sinensis flowers and their antibacterial activity. J Nanotechnol 1–6. https://doi.org/10.1155/2022/5474645
27. Demirezen DA, Yilmaz D, Yılmaz Ş (2018) Green synthesis and characterization of iron nanoparticles using Aesculus hippocastanum seed extract. Int J Adv Sci Eng Technol 6:2321–8991. IJASEAT-IRAJ-DOIONLINE-12665
28. Ahmmad B, Leonard K, Islam MS, Kurawaki J, Muruganandham M, Ohkubo T, Kuroda Y (2013) Green synthesis of mesoporous hematite (α-Fe2O3) nanoparticles and their photocatalytic activity. Adv Powder Technol 24(1):160–167. https://doi.org/10.1016/j.apt.2012.04.005
29. Lassoued A, Lassoued MS, Dkhil B, Ammar S, Gadri A (2018) Synthesis, photoluminescence and magnetic properties of iron oxide (α-Fe2O3) nanoparticles through precipitation or hydrothermal methods. Physica E 101:212–219. https://doi.org/10.1016/j.physe.2018.04.009
30. Jagathesan G, Rajiv P (2018) Biosynthesis and characterization of iron oxide nanoparticles using Eichhornia crassipes leaf extract and assessing their antibacterial activity. Biocatal Agric Biotechnol 13:90–94. https://doi.org/10.1016/j.bcab.2017.11.014
31. Velsankar K, Parvathy G, Mohandoss S et al (2022) *Celosia argentea* leaf extract-mediated green synthesized iron oxide nanoparticles for bio-applications. J Nanostruct Chem 12:625–640. https://doi.org/10.1007/s40097-021-00434-5
32. Arokiyaraj S, Saravanan M, Prakash NU, Arasu MV, Vijayakumar B, Vincent S (2013) Enhanced antibacterial activity of iron oxide magnetic nanoparticles treated with Argemone mexicana L. leaf extract: an in vitro study. Mater Res Bullet 48(9):3323–3327. https://doi.org/10.1016/j.materresbull.2013.05.059
33. Ge X, Cao Z, Chu L (2022) The antioxidant effect of the metal and metal-oxide nanoparticles. Antioxidants 11(4):791. https://doi.org/10.3390/antiox11040791
34. Thukkaram M, Sitaram S, Subbiahdoss G (2014) Antibacterial efficacy of iron-oxide nanoparticles against biofilms on different biomaterial surfaces. Int J Biomater. https://doi.org/10.1155/2014/716080
35. Priya MR, Subashini R, Kumar PS, Deepadharshini A, Sree MM, Murugan K, Sumathi M (2022) Assessment of in vitro biopotency of bioderived silver nanoparticles from Aegle marmelos (L.) fruit extract. Appl Nanosci 1–1. https://doi.org/10.1007/s13204-022-02619-y
36. Abou-Elella F, Hanafy EA, Gavamukulya Y (2016) Determination of antioxidant and anti-inflammatory activities, as well as in vitro cytotoxic activities of extracts of Anastatica hierochuntica (Kaff Maryam) against HeLa cell lines. J Med Plants Res 10(7):77–87. https://doi.org/10.5897/JMPR2015.6030
37. Erdoğan Ö, Paşa S, Demirbolat GM, Çevik Ö (2021) Green biosynthesis, characterization, and cytotoxic effect of magnetic iron nanoparticles using Brassica Oleracea var capitata sub var rubra (red cabbage) aqueous peel extract. Turk J Chem 45(4):1086–1096. https://doi.org/10.3906/kim-2102-2
38. Sharma P, Dhiman S, Kumari S, Rawat P, Srivastava C, Sato H, Akitsu T, Kumar S, Hassan I, Majumder S (2019) Revisiting the physiochemical properties of hematite (α-Fe2O3) nanoparticle and exploring its bio-environmental application. Mater Res Exp 6(9):095072. https://doi.org/10.1088/2053-1591/ab30ef